PHOTON CORRELATION SPECTROSCOPIC STUDY OF THE SIZE DISTRIBUTION OF PHOSPHOLIPID VESICLES

J. GOLL AND F. D. CARLSON
Department of Biophysics, Johns Hopkins University, Baltimore, Maryland 21217

Y. BARENHOLZ, B. J. LITMAN, AND T. E. THOMPSON
Department of Biochemistry, University of Virginia School of Medicine, Charlottesville, Virginia 22908

ABSTRACT The dependence of phospholipid vesicle size on lipid composition is investigated by photon correlation spectroscopy. For each lipid composition prolonged ultracentrifugation was used to isolate a nearly uniform population of minimum-sized vesicles. The residual size variations in the samples were sufficient to cause polydispersity that made comparisons between samples difficult. Analyses of the data by the method of cumulants and by a method for approximating the particle size distributions directly are presented. The latter method made possible unambiguous comparisons that revealed small but systematic dependences of vesicle size on composition in vesicles containing mixtures of egg phosphatidylcholine and phosphatidylethanolamine, egg phosphatidylcholine and beef brain sphingomyelin, and in single lipid vesicles of egg phosphatidylcholine, dioleylphosphatidylcholine, and beef brain sphingomyelin. These size dependences are quantified within the resolution limits of the technique and their implications are discussed.

INTRODUCTION

Studies of phospholipid vesicles, both as single and multicomponent systems, have served as a means of elucidating the role of specific factors in determining the properties of biological membranes (1–3). These systems have been used to study protein-phospholipid interactions and for the delivery of biologically active molecules to target cells both in vitro and in vivo (4). A variety of such studies have demonstrated a dependence of phospholipid bilayer properties on the vesicle radius of curvature (5–8), thus requiring vesicle size information for a unique interpretation of the data. Although several physical techniques have been used to determine phospholipid vesicle size, very little information is currently available that would allow a systematic evaluation of the effect of composition on phospholipid vesicle radius. An initial study to provide such information is reported in this paper.

Phospholipid vesicles made by sonication of an aqueous dispersion of lipids can be separated by molecular sieve chromatography (9) or by differential ultracentrifugation (10) into two fractions. The major fraction, containing 70% or more of the phospholipid, consists of a relatively uniform population of small, single bilayer vesicles; the other fraction consists of larger structures that are very heterogeneous in size. In this study, the effect of lipid composition on the average size and size distribution of the small vesicle fraction was investigated by photon correlation spectroscopy. This technique has been used before to study vesicle size as well as aggregation and fusion (10–14). Assuming the vesicles are nearly spherical, the mean Stokes' radius determined from the photon correlation data relates directly to the curvature of the bilayer wall. A small, but well-defined dependence of vesicle radius on lipid composition is reported here. This result may have a bearing on the structure-function relations in biological membranes, which frequently exhibit folded regions with radii of curvature comparable to the radii of these small vesicles (5).

MATERIALS AND METHODS

Phospholipid Preparation

Bovine brain sphingomeylin, [^{3}H]phosphatidylcholine from rat liver, egg phosphatidylcholine, and egg phosphatidylethanolamine were prepared as previously described (7,10). Dioleylphosphatidylcholine was synthesized and purified as described by Lentz et al. (15). The purity of the lipids was established by thin-layer chromatography at micromole loadings (7,15).

Preparation of Phospholipid Vesicles

Individual phospholipids or binary mixtures of phospholipids were first dissolved in benzene and then lyophilized to remove all traces of organic solvent. The dry phospholipid was then suspended in either 50-mM KCl or 100-mM NaCl prepared from de-ionized water which was first distilled over alkaline $KMnO_4$ and then glass redistilled. Vesicle disper-

Dr. Goll's current address is Texas Instruments, Inc., Dallas, TX 75265.

Dr. Barenholtz completed part of the work for this paper at the Department of Biochemistry, Hebrew University School of Medicine, Jerusalem, Israel.

sions were prepared by sonication of these aqueous suspensions under nitrogen at temperatures above the phase transition of the phospholipid using a Heat Systems Sonifier (W-350 Heat Systems Ultrasonics, Inc., Plainview, NJ). The details of this procedure are given elsewhere (10). Following sonication, a dispersion of small unilamellar vesicles was prepared by differential ultracentrifugation. This method, which has been described in detail in a previous publication (10), has several advantages over the original molecular sieve chromatography method developed by Huang (9). The most important of these advantages for this photon correlation spectroscopy study is the absence of materials that are shed by the molecular sieve matrix and strongly contribute to low-angle scattering and the higher vesicle concentration in the final solutions.

For the work reported in this paper, appropriate centrifugation conditions for the various vesicle systems were determined empirically as follows. Samples of a given lipid vesicle dispersion were centrifuged for successively longer periods of time until cumulant analysis (16) of the correlation data showed no further increase in the intensity-averaged diffusion coefficient. This centrifugation time was then used to prepare systems of similar lipid composition. Centrifugation was performed in a Beckman L5-50 ultracentrifuge using a Beckman Ti-65 fixed-angle rotor at 50,000 rpm, 20°C (Beckman Instruments, Inc., Palo Alto, CA). Samples were stored at 4°C. Some showed a slow time-dependent decrease in the average value of the diffusion coefficient determined by cumulant analysis. Before additional work with these samples was carried out, the diffusion coefficient was restored to its original average valued by repetition of the centrifugation procedure.

Photon Correlation Spectroscopy

Measurements were carried out using a serial digital autocorrelator interfaced with a Nova 2 minicomputer (Data General Corporation, Southboro, MA) and an optical arrangement described previously (17). Detailed descriptions of the methods of data collection and analysis are given elsewhere (11).

Determination of Phospholipid Concentrations

The total concentration of phospholipid in dispersions was determined by the method of Bartlett (18). Determination of the total phosphatidylethanolamine content of vesicles and the fraction of this phospholipid present in the outer vesicle surface was carried out using 2,4,6-trinitrobenzene sulfonate as described by Barenholz et al. (10). The mole ratio of sphingomyelin to phosphatidylcholine in vesicles formed from mixtures of these phospholipids was determined from the total lipid phosphorus and the content of [^{3}H]phosphatidylcholine. Turbidity of vesicle dispersions was measured in a 1-cm cell at 300 nm using a Gilford 240 spectrophotometer (Gilford Instrument Laboratories, Inc., Oberlin, OH).

RESULTS

Vesicle dispersions, prepared as described above, exhibited a small, but detectable, polydispersity as analyzed by photon correlation spectroscopy. Initial analysis of data utilized the method of cumulants (16) and is summarized in Table I. Unambiguous comparisons, including determinations of minimum vesicle size, were desired for the various composition vesicle samples. Most samples contained a small fraction of larger, non-Rayleigh scatterers as shown by the dependence of the diffusion coefficient estimate (derived from the first moment) on scattering angle. All samples had nonzero second moments, indicating a mixture of particle sizes. For some lipid compositions the z-averaged diffusion coefficient calculated from the first moment was not satisfactorily reproducible when nominally equivalent preparations were used. This showed the familiar sensitivity of photon correlation spectroscopic experiments to small changes in the large particle content of a preparation. In spite of these difficulties, it is possible to suggest trends in the dependence of vesicle radius on composition, based on the data in Table I alone. However, the minimum vesicle size is obscured by the z-averaging over a distribution that includes unknown large particle contaminants. Many different size distributions are consistent with all the data in Table I. For example, it is difficult to distinguish a shift toward larger size in all particles in a sample from a shift in only some. Finally, the distribution function describing the actual vesicle size distribution obviously does not depend on scattering angle or any other detail of the photon correlation spectroscopy experimental procedure. The estimates of these moments provided by the method of cumulants shown in Table I vary significantly with scattering angle. These variations arise because the angle-dependent scattering intensities of the non-Rayleigh scatterers in the solution are not accounted for in the cumulant method.

These difficulties in interpretation were overcome by utilizing a method for approximating the particle size distribution functions directly (11,19). The distribution functions were approximated by piecewise-linear functions called first-order splines. Two features of this method, the use of unusually extensive light-scattering data and the imposition of constraints on the distribution functions using information derived from other studies, made it possible to define the distribution functions with sufficient resolution to allow clear comparisons between different samples.

The distributions were based on simultaneous fits to data gathered at four or five different scattering angles. The population of vesicles was modeled as a mixture of spherical shells of varying radius, with 40-Å wall thickness (9). As detailed by Goll and Stock (11), the Rayleigh-Gans form factor for spherical shells was used. It was assumed that the refractive indices of the fluids inside and outside the vesicles were the same. Under these conditions the refractive index does not enter into the calculation. This follows from the fact that, whereas the absolute intensity scattered by a given vesicle depends on the refractive index, the relative intensity, which is all that enters into our calculation (11), is independent of refractive index. It should be noted that modeling the vesicles as spheres rather than spherical shells led to fits to the data only slightly poorer than those presented here. Therefore the use of spherical shells in the model is not critical.

The distributions are accompanied by a statistical analysis that yields a standard deviation for each distribution parameter (11). This analysis demonstrates that the differences between samples are statistically significant. By determining the distributions directly, the problems described above, which stem from the sensitivity of photon

TABLE I

CUMULANT ANALYSIS OF PHOSPHOLIPID VESICLES AT VARIOUS COMPOSITION

100% Egg PC*						
Angle	22.01°	32.02°	59.98°	90.00°	118.82°	151.18°
$\bar{\Gamma}/q^2$‡	1.90 ± 0.04	2.01 ± 0.02	1.97 ± 0.06	2.02 ± 0.02	2.01 ± 0.01	2.03 ± 0.02
Q§	0.154 ± 0.022	0.145 ± 0.029	0.103 ± 0.015	0.041 ± 0.022	0.022 ± 0.002	−0.023 ± 0.032
25% Spm:75% egg PC						
Angle	22.01°	28.81°	61.19°	90.00°	118.81°	
$\bar{\Gamma}/q^2$	1.407 ± 0.022	1.479 ± 0.019	1.588 ± 0.02	1.618 ± 0.005	1.617 ± 0.0007	
Q	0.326 ± 0.016	0.246 ± 0.038	0.161 ± 0.014	0.134 ± 0.004	0.106 ± 0.009	
75% Spm: 25% egg PC						
Angle		28.81°	61.19°	90.00°	118.81°	
$\bar{\Gamma}/q^2$		1.375 ± 0.009	1.437 ± 0.02	1.439 ± 0.010	1.467 ± 0.017	
Q		0.200 ± 0.025	0.125 ± 0.019	0.072 ± 0.009	0.089 ± 0.030	
100% Spm						
Angle	22.01°	28.81°	61.19°	90.00°	118.81°	
$\bar{\Gamma}/q^2$	1.27 ± 0.04	1.47 ± 0.01	1.535 ± 0.015	1.536 ± 0.005	1.562 ± 0.025	
Q	0.308 ± 0.016	0.218 ± 0.023	0.155 ± 0.012	0.115 ± 0.016	0.125 ± 0.006	
DOPC						
Angle	22.01°	28.81°	61.19°	90.00°	118.81°	
$\bar{\Gamma}/q^2$	1.27 ± 0.006	1.351 ± 0.004	1.410 ± 0.007	1.373 ± 0.013	1.419 ± 0.006	
Q	0.201 ± 0.033	0.191 ± 0.006	0.168 ± 0.006	0.141 ± 0.008	0.126 ± 0.014	
10% PE: 90% PC						
Angle	22.01°	28.81°	61.19°	90.00°	118.81°	
$\bar{\Gamma}/q^2$	1.713 ± 0.013	1.773 ± 0.024	1.738 ± 0.008	1.765 ± 0.010	1.727 ± 0.030	
Q	0.170 ± 0.028	0.124 ± 0.018	0.132 ± 0.019	0.100 ± 0.005	0.121 ± 0.006	
25% PE: 75% PC						
Angle	22.01°	28.81°	61.19°	90.00°	118.81°	
$\bar{\Gamma}/q^2$	1.597 ± 0.007	1.633 ± 0.022	1.618 ± 0.006	1.574 ± 0.023	1.571 ± 0.022	
Q	0.170 ± 0.010	0.166 ± 0.009	0.127 ± 0.008	0.072 ± 0.015	0.111 ± 0.012	
50% PE: 50% PC						
Angle	22.01°	28.81°	61.19°	96.00°	118.81°	
$\bar{\Gamma}/q^2$	1.288 ± 0.017	1.331 ± 0.012	1.408 ± 0.011	1.389 ± 0.013	1.369 ± 0.016	
Q	0.319 ± 0.012	0.198 ± 0.013	0.110 ± 0.015	0.061 ± 0.010	0.053 ± 0.013	

*PC, phosphatidylcholine; PE, phosphatidylethanolamine; Spm, sphingomyelin; DOPC, dioleylphosphatidylcholine.

‡$\bar{\Gamma}$ is the intensity-weighted average of the decay constant = $D(R)q^2$ (θ).

§$Q = M_2/\bar{\Gamma}^2$, where M_2 is the intensity-weighted average value of $(\Gamma - \bar{\Gamma})^2$.

correlation spectroscopy to large particle contaminants, were minimized. In particular the estimate of minimum particle size was made more reliable by eliminating the strong effect of large particle on z-averaging. Therefore, the confidence that can be placed in comparisons between the samples is greater than that merited by comparisons based on cumulants alone.

Several of the samples discussed here exhibited significantly more polydispersity than the case treated in detail by Goll and Stock (11). Nevertheless, good fits to the data were obtained with all systems studied, as indicated by values near 1 of χ^2 per degree of freedom. For each system examined, the particle size distribution is presented as a normalized mass density $M(R)$. The distribution is approximated by a piecewise-linear function with turning points at selected radii called knots. Only four or five independent parameters, corresponding to seven or eight knots and six or seven linear sections of the distribution, could be determined independently (11). Therefore the distributions are based on seven or eight knots in all cases.

As discussed by Goll and Stock (11), the localized details of the distributions depend to an extent on the selection of the knots used in defining the distributions, but important general features of the distributions are independent of the selected knots. This is illustrated in Fig. 1*A* and *B*. Shown in the figures are the mass density functions for two samples, egg phosphatidylcholine (solid lines) and 75% egg phosphatidylcholine plus 25% egg phosphatidylethanolamine (dashed lines). Fig. 1*A* shows the fits using a set of knots anchored at 100 Å; Fig. 1*B* shows the fits to the same data using a set of knots with a 90-Å lower limit. Note that χ^2 per degree of freedom was essentially the

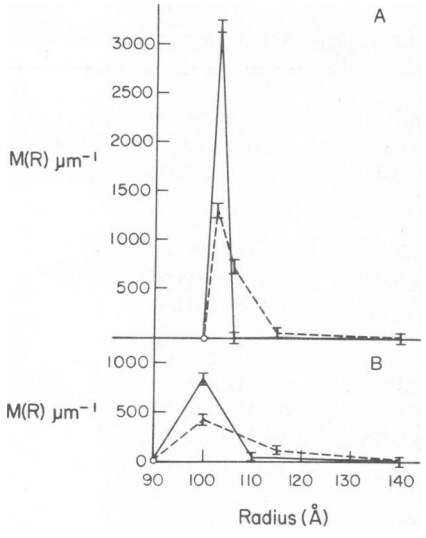

FIGURE 1 (*A*) The normalized mass density functions, $M(R)$, plotted against the radius, R, for egg phosphatidylcholine (—) and 75% egg phosphatidylcholine and 25% egg phosphatidylethanolamine (---) using set of knots with 100-Å lower limit. (*B*) Mass density functions for the same samples as in *A* using set of knots with 90-Å lower limit. Note that only $R < 140$ Å is included here.

same for all four fits. The influence of the selected knots can be seen by comparing the solid or dashed lines in *A* and *B*. This comparison shows that highly localized features (such as the distribution width at half amplitude) cannot be resolved with the current technique. Less localized features, however, do not depend significantly on the locations of the knots. For example, provided there is a knot located at 140 Å, the total fraction of mass found in vesicles with radius <140 Å for a given sample does not depend on the selection of knots, and this parameter does vary from sample to sample.

All distributions used to make comparisons of samples of differing lipid compositions are based on knots similar to those of Fig. 1*B*. A minimum radius of 90 Å is used in all cases.[1] Because the various mass distributions differ, it was necessary to vary the choices of knots somewhat from sample to sample in order to optimize the fits to the data.

For simplicity, comparisons among the samples are made in terms of mass-weighted average radius $\overline{R}$ and root-mean-square deviation from this average $[(R - \overline{R})^2]^{1/2}$. In all cases these comparisons are consistent with the more extensive information about the samples provided by the distributions themselves. As the distributions are available, any weighting function desired could be used in calculating moments. Mass weighting was selected for the following three reasons: these moments, unlike intensity-weighted moments, are consistent with all the data gathered at all scattering angles; they are relatively insensitive to the influence of small quantities of large particle contaminants; and they are directly comparable to average radii derived from sedimentation coefficient measurements.

The normalized mass density functions for vesicles of various compositions are given in Table II. For each vesicle system, the knot positions R, the values of the normalized mass density functions $M(R)$ at these positions, and the standard deviations σ are listed. The units of $M(R)$ and σ are μm^{-1}. The complete distribution functions are obtained by connecting the points $[R,M(R)]$ sequentially by straight lines as illustrated in Figs. 1 and 2. The mass-weighted average vesicle radii and standard deviations about these averages are presented for single component vesicles, Table III, and for vesicles composed of mixtures of two phospholipids, Table IV.

The normalized mass density functions for three single-component vesicle systems, egg phosphatidylcholine, dioleylphosphatidylcholine, and beef brain sphingomyelin, are plotted in Fig. 2. Vesicles prepared from egg phosphatidylcholine exhibit both the smallest average radius and the narrowest distribution function. Both bovine brain sphingomyelin vesicles and dioleylphosphatidylcholine vesicles exhibit significantly higher average radii and distribution breadth.

In the phosphatidylethanolamine/phosphatidylcholine and the sphingomyelin/phosphatidylcholine systems, both the average vesicle radius and the breadth of the distribution function increase as the mole fraction of the minority component increases toward 50%. It is impossible to form stable phosphatidylethanolamine/phosphatidylcholine vesicles with >70 mol % phosphatidylethanolamine (7). Sphingomyelin/phosphatidylcholine vesicles form over the entire concentration range. Among the compositions investigated for this system, the highest mean vesicle radius occurs at 75 mol % sphingomyelin.

DISCUSSION

Our results may be compared in two cases with previously published determinations of mean particle size. The value of the average radius of egg phosphatidylcholine vesicles reported here agrees well with the value of 105 Å reported by Huang and Lee (20), calculated from diffusion coefficient data obtained in the ultracentrifuge. The result obtained here for sphingomyelin vesicles differs substantially from the value of 247 ± 10 Å, reported by Cooper et al. (21) for sonicated vesicles prepared from a spinal cord sphingomyelin fraction (3) and determined by photon correlation spectroscopy. This disagreement can probably be attributed to the differences in lipid composition of the two preparations (21), the use in the current study of prolonged ultracentrifugation to obtain minimum-sized vesicles, and the difference between the mass-weighted averages utilized here and the intensity-weighted averages used by Cooper et al. (21).

The mass-averaged moments derived from the distributions proved to be sufficient to define the major differences

[1]The minimum radius of 90 Å for a lipid vesicle is based on the theoretical calculation of Israelachvili et al. (6).

TABLE II
MASS DENSITY DISTRIBUTIONS FOR VESICLES OF VARIOUS COMPOSITION

Egg PC*							
Radius, Å	90	100	110	140	300	800	2,000
$M(R)$, μm^{-1}	0	857	58	0.26	0.030	1.16×10^{-4}	0
σ, μm^{-1}		50	22	0.26	0.005	1.16×10^{-4}	
Spm							
Radius, Å	90	100	115	140	300	800	2,000
$M(R)$, μm^{-1}	0	3.1	455	0.30	0.13	2.5×10^{-3}	0
σ, μm^{-1}		3.1	10	0.2	0.01	3.0×10^{-4}	
DOPC							
Radius, Å	90	110	130	160	300	800	2,000
$M(R)$, μm^{-1}	0	280	75.5	16.6	2.3×10^{-3}	4.8×10^{-8}	0
σ, μm^{-1}		14	7.5	0.6	2.3×10^{-3}	2×10^{-4}	
10% Egg PE: 90% Egg PC							
Radius, Å	90	100	110	120	150	300	900
$M(R)$, μm^{-1}	0	658	165	27	6.63	1.0×10^{-3}	0
σ, μm^{-1}		110	165	27	0.51	1.0×10^{-3}	
25% PE: 75% PC							
Radius, Å	90	100	115	140	300	800	2,000
$M(R)$, μm^{-1}	0	445	128	7.5	8.0×10^{-4}	1.85×10^{-3}	0
σ, μm^{-1}		30	19	0.3	8.0×10^{-4}	1.0×10^{-4}	
50% PE: 50% PC							
Radius, Å	90	110	130	160	300	800	2,000
$M(R)$, μm^{-1}	0	28	315	6.7	0.061	4.9×10^{-3}	0
σ, μm^{-1}		28	29	1.5	0.010	1.0×10^{-3}	
25% Spm: 75% PC							
Radius, Å	90	100	115	140	300	800	2,000
$M(R)$, μm^{-1}	0	603	25	7.9	0.115	6.6×10^{-3}	0
σ, μm^{-1}		52	25	0.1	0.115	2.0×10^{-4}	
75% Spm: 25% PC							
Radius, Å	90	100	115	130	160	300	800	2,000
$M(R)$, μm^{-1}	0	74.5	130	278	5.7	3.5×10^{-3}	8.0×10^{-3}	0
σ, μm^{-1}		40	120	66	0.7	3.5×10^{-3}	2.0×10^{-4}	

*PC, phosphatidylcholine; PE, phosphatidylethanolamine; Spm, sphingomyelin; DOPC, dioleylphosphatidylcholine.

among the samples. However, we emphasize that the distributions reveal distinctions beyond those indicated by the first two moments. Consider, for example, the two samples dioleylphosphatidylcholine and 75% sphingomyelin/25% phosphatidylcholine. On the basis of the cumulant analysis (Table I) and the mass-averaged moments (Tables III and IV), we have determined that these samples are very similar. The greatest distinction is in the second cumulants at high scattering angles. Table II shows that the dioleylphosphatidylcholine distribution has a peak at a significantly lower radius than the 75% sphingomyelin distribution and a higher value of $M(R)$ for vesicles of intermediate size ($150 < R < 300$ Å). This difference could not be determined from the first two moments alone. The third moment, which would be requried in this case to reveal the distinction based on moments alone, cannot be determined meaningfully using cumulants but could be determined from the distribution. Note that even if the first two moments of the two samples had been identical, differences in the distributions of the kind illustrated here could be present.

There are marked differences in the radii of vesicles comprised of the three lipids examined in this study.

TABLE III
MEAN VESICLE RADIUS FOR SINGLE COMPONENT SYSTEMS

System*	Mass-weighted average radius (Å)	
	$\bar{R}_m$	$\sqrt{(R - \bar{R})^2}$
Egg PC*	104.0 ± 0.7	22.8 ± 0.9
Spm	124.4 ± 0.6	48 ± 2
DOPC	140.5 ± 0.5	56.2 ± 1

*PC, phosphatidylcholine; Spm, sphingomeylin; DOPC, dioleylphosphatidylcholine.

TABLE IV
MEAN VESICLE RADIUS FOR SYSTEMS COMPRISED OF TWO PHOSPHOLIPID COMPONENTS

System*	Composition	Mass-weighted average radius (Å) $\bar{R}_m$	$\sqrt{(R - \bar{R})^2}$
PE/PC*	10/90	114.6 ± 0.5	35.8 ± 1.3
	25/75	121.9 ± 0.3	43.6 ± 0.3
	50/50	143.7 ± 0.7	50.7 ± 2.0
Spm/PC	25/75	119 ± 3	60 ± 5
	75/25	139 ± 2	52 ± 1

*PC, phosphatidylcholine; PE, phosphatidylethanolamine; Spm, sphingomyelin.

Values of the radii appear to correlate inversely with the acyl chain heterogeneity of the preparation. Both egg phosphatidylcholine and bovine brain sphingomyelin are comprised of mixtures of molecules differing only in their acyl chain composition. The heterogeneity of acyl chains is, however, considerably greater in egg phosphatidylcholine, which contains two acyl chains per molecule, than it is in sphingomyelin, which contains only a single variable acyl group (22). Analyses of acyl chain composition of these two preparations also shows a greater range for egg phosphatidylcholine than for bovine brain sphingomyelin (22). In contrast to these two natural preparations, the synthetic dioleylphosphatidylcholine is a single molecular species. The basis for the inverse correlation between vesicle radius and acyl chain heterogeneity may rest on the fact that as the vesicle radius decreases, the molecular packing constraints in the two bilayer faces become more restrictive. The additional degrees of freedom gained by increased heterogeneity of acyl chains may make it possible to meet these constraints at a smaller radius.

The data in Table II indicate that the breadth of the distribution function for vesicle radius increases in the order egg phosphatidylcholine less than bovine brain sphingomyelin less than dioleylphosphatidylcholine. The molecular basis for this correlation is not immediately apparent.

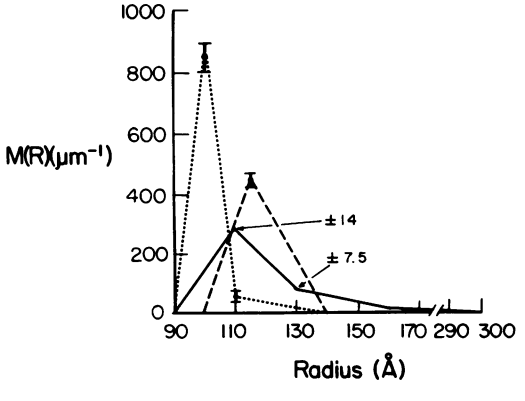

FIGURE 2 The normalized mass density functions, $M(R)$, plotted against the radius, R, for vesicles prepared from egg phosphatidylcholine (····), dioleylphosphatidylcholine (—), and beef brain sphingomyelin (---).

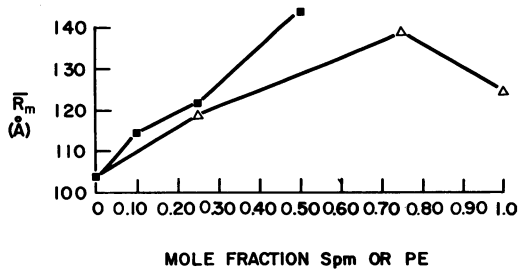

FIGURE 3 The mean vesicle radius R_m plotted as a function of composition for vesicles composed of egg phosphatidylcholine and phosphatidylethanolamine (■) or sphingomyelin (△). Spm, sphingomyelin; PE, phosphatidylethanolamine.

In the systems composed of mixtures of two phospholipids of different types both average vesicle size and distribution breadth increase as the mole fraction of the minor component increases. This is illustrated in Figs. 3 and 4. The increase in size with increasing minority component is apparently consistent with the positive deviations from ideal mixing exhibited by most binary phospholipid systems in bilayer form (8). Because the mean vesicle radius increases with increasing content of the minor component, it seems possible that the breadth of the distribution function for a given composition system simply reflects a distribution of individual vesicle compositions. Litman (7) has, however, shown for vesicles made from various mixtures of phosphatidylethanolamine and phosphatidylcholine that the compositions of all vesicle fractions obtained on molecular sieve chromatography of a given system are essentially identical. These same systems exhibit a marked distribution of sedimentation coefficients in the ultracentrifuge (7) that must be related only to the heterogeneity in vesicle size as deduced from the proton correlation spectroscopic data. Similar molecular sieve and sedimentation data obtained for sphingomyelin/phosphatidylcholine mixtures (unpublished observations) lead to the same conclusion; that is, that the size distribution is not the result of compositional variations among vesicles.

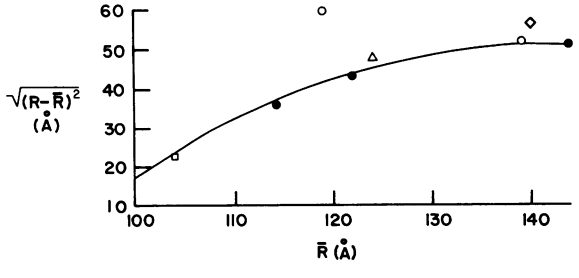

FIGURE 4 Plot of the average deviation, $\sqrt{(R - R)^2}$, vs. the mass-weighted average radius for vesicles composed of egg phosphatidylcholine (□), sphingomyelin (△), dioleylphosphatidylcholine (◇), mixtures of egg phosphatidylcholine/phosphatidylethanolamine (●) and phosphatidylcholine/sphingomyelin (○).

At all compositions studied, the phosphatidylethanolamine/phosphatidylcholine system is in the liquid crystalline state. Such is not the case for vesicles comprised of sphingomyelin/phosphatidylcholine. The phase diagram for this system has been determined from fluorescence polarization data obtained using the hydrophobic probe 1,6 diphenyl-1,3,5 hexatriene (3). It is apparent that at 20°C, the temperature of the photon correlation spectroscopic measurement, this system consists of both gel and liquid crystalline phases between ~20 and 50 mol % phosphatidylcholine (3). Above 50 mol % of this component, the system is completely liquid crystalline at 20°C. The complex phase behavior of vesicles formed from mixtures of these two lipids also causes a simple thermodynamic parameter such as the apparent specific volume of the total lipid to deviate markedly from ideality (3). Thus, at 20°C the mixing volume of these two lipid components is substantially greater than simple additivity of the individual molar volumes of the two components. It appears that this nonideal behavior is directly reflected in the variation of mean vesicle radius with composition. It thus seems reasonable to conclude that the minimum vesicle radius that is achieved by sonication reflects the mixing properties of the component lipids.

The single lamellar vesicles examined in this study were formed by sonication of aqueous phospholipid dispersions. Although other procedures may be used to form similar vesicles (23), those generated by sonication appear to have minimum radii. Thus vesicles generated in this way are a special case in which the packing differences exhibited by individual molecules are most exaggerated because of the minimum bilayer radii. We have no evidence that single lamellar vesicles formed by other procedures have properties similar to those presented in this paper.

This work was supported by United States Public Health Service grants GM-14628, HL-17576, EY-00548, GM-05181, AM-12803, AM-16315, National Science Foundation grant PCM-8012028, and US-Israel Binational Science Foundation grant 1688.

Received for publication 11 April 1981 and in revised form 20 October 1981.

REFERENCES

1. Lee, A. G. 1975. Functional properties of biological membranes: a physical-chemical approach. *Prog. Biophys. Mol. Biol.* 29:3–56.
2. Seelig, J., and A. Seelig. 1980. Lipid conformation in model membranes and biological membranes. *Q. Rev. Biophys.* 13:19–62.
3. Barenholz, Y., and T. E. Thompson. 1980. Sphingomyelins in bilayers and biological membranes. *Biochim. Biophys. Acta.* 604:129–158.
4. Szoka, F., Jr., and D. Papahadjopoulos. 1980. Comparative properties and methods of preparation of lipid vesicles (liposomes). *Annu. Rev. Biophys. Bioeng.* 9:467–508.
5. Thompson, T. E., C. Huang, and B. J. Litman. 1974. Bilayers and biomembranes: compositional asymmetries induced by surface curvature. *In* The Cell Surface in Development. A. A. Moscona, editor. John Wiley & Sons, Inc., New York. 1–16.
6. Israelachvili, J. N., S. Marcelja, and R. G. Horn. 1980. Physical principles of membrane organization. *Q. Rev. Biophys.* 13:121–200.
7. Litman, B. J. 1973. Lipid model membranes. Characterization of mixed phospholipid vesicles. *Biochemistry.* 12:2545–2554.
8. Thompson, T. E., B. R. Lentz, and Y. Barenholz. 1977. A calorimetric and fluorescent probe study of phase transitions in phosphatidylcholine liposomes. *In* Biochemistry of Membrane Transport. G. Smenya and E. Carafoli editors. Springer-Verlag, Berlin. 47–71.
9. Huang, C. 1969. Studies on phosphatidylcholine vesicles: formation and physical characteristics. *Biochemistry.* 8:344–352.
10. Barenholz, Y., D. Gibbes, B. J. Litman, J. Goll, T. E. Thompson, and E. D. Carlson. 1977. A simple method for the preparation of homogeneous phospholipid vesicles. *Biochemistry.* 16:2806–2810.
11. Goll, J. H., and G. B. Stock. 1977. Determinations by photon correlation spectroscopy of particle size distributions in lipid vesicle suspensions. *Biophys. J.* 19:265–273.
12. Pownall, H. J., J. B. Massey, S. K. Kusseron, and A. M. Gotto, Jr. 1978. Kinetics of lipid protein interaction: interaction of apolipoprotein A-I from human plasma high density lipoproteins with phosphatidylcholines. *Biochemistry.* 17:1183–1188.
13. Sut, S. T., E. P. Day, J. T. Ho. 1978. Temperature dependence of calcium induced fusion of sonicated phosphatidylserine vesicles. *Proc. Natl. Acad. Sci. U. S. A.* 75:4325–4328.
14. Chen, F. C., A. Chreszczyk, and B. Chu. 1977. Quasielastic laser light scattering of monolayer vesicles. *J. Chem. Phys.* 66:2237–2245.
15. Lentz, B. R., Y. Barenholz, and T. E. Thompson. 1976. Fluorescence depolarization studies of phase transitions and fluidity in phospholipid bilayers. I. Single component phosphatidylcholine liposomes. *Biochemistry.* 15:4521–4528.
16. Koppel, D. E. 1972. Analysis of macromolecular polydespersity in intensity correlation spectroscopy: the method of cumulants. *J. Chem. Phys.* 57:4814–4820.
17. Carlson, F. D., B. Bonner, and A. Fraser. 1972. Intensity fluctuation autocorrelation studies of resting and contracting frog sartorius muscle. *Cold Spring Harbor Symp. Quant. Biol.* 37:389.
18. Bartlett, G. R. 1959. Phosphorus assay in column chromatography. *J. Biol. chem.* 234:466–471.
19. Stock, G. B. 1976. Application of splines to the calculation of bacterial swimming speed distributions. *Biophys. J.* 16:535–549.
20. Huang, C., and L. P. Lee. 1973. Diffusion studies in phosphatidylcholine vesicles. *J. Am. Chem. Soc.* 95:234–239.
21. Cooper, V. G., S. Yedgar, and Y. Barenholz, 1974. Diffusion coefficients of mixed micelles, Triton X-100 and sphingomyelin and of sonicated liposomes measured by autocorrelation spectroscopy of Rayleigh scattered light. *Biochim. Biophys. Acta.* 363:86–97.
22. White, D. A. 1973. Phospholipid composition of mammalian tissues. *In* Form and Functions of Phospholipids. G. B. Ansell, J. N. Hawthorne, and R. M. C. Dawson, editors. Elsevier/North Holland, New York. 441.
23. Pagano, R. E., and J. N. Weinstein. 1978. Interactions of liposomes with mammalian cells. *Annu. Rev. Biophys. Bioeng.* 7:435–468.